Applying an adaptive subtraction technique to suppress the acquisition footprint pattern as seen on geometric attributes: A Red Fork Formation case study.

*Yavuz Ozan ELIS *, The University of Oklahoma*
Kurt J. Marfurt, The University of Oklahoma, USA.

Downloaded 01/29/13 to 129.15.127.245. Redistribution subject to SEG license or copyright; see Terms of Use at http://library.seg.org/

Summary

The Middle Pennsylvanian Red Fork Formation is one of the most significant and widespread producing zones in northern Oklahoma. The Red Fork Formation consists of incised valley fill, which formed during changes of sea level. One of the biggest challenges of our legacy 3D dataset acquired in the mid 1990s over the Red Fork Formation is acquisition footprint, which contaminates the data and may mislead the interpretation. In order to delineate the subtle features and to distinguish channel edges from linear artifacts, it is important to remove the acquisition footprint from the data. We improved upon the data quality by reprocessing the original field data with the express goal of reducing the acquisition footprint on the final image. After reprocessing the data, we applied an adaptive subtraction footprint suppression workflow to the processed data and evaluated the effectiveness of this workflow by computing geometric attributes before and after acquisition footprint suppression.

Introduction

3D seismic data are adversely affected by various kinds of noise that needs to be addressed during the seismic processing. Though seismic processing readily attenuates random noise from the seismic data, coherent noise coupled to the acquisition is more challenging. Acquisition footprint is one type of challenging noise that masks important details which are critical to the identification of key reservoir properties. Marfurt et al. (1998) define acquisition footprint as "any pattern of noise that is highly correlated to the geometric distribution of sources and receivers on the earth's surface." Non-uniform offset and azimuth distribution across bins, non-uniform backscattered noise suppression, incorrect geometry, inaccurate velocities, and migration operator aliasing can all give rise to acquisition footprint. Our 3D legacy dataset acquired over the Red Fork Formation suffer from acquisition footprint and effect of this footprint is exacerbated by modern seismic attributes. To address this problem, we have reprocessed the seismic data volume by carefully examining each processing step. Once the signal to noise ratio has been boosted, we have analyzed the effect of acquisition footprint on most-positive principal curvature, coherent energy, and the coherent energy gradient. Once the footprint pattern has been characterized, we applied the $k_x - k_y$ transform adaptive subtraction technique proposed by Falconer and Marfurt (2008) to the processed data and recomputed the attributes.

Description of the data and Geological framework

The seismic surveys were acquired by Amoco during three different stages from 1993 to 1996 and were finally merged into a 136 mi^2 (348 km^2) survey, which is located in the eastern part of the Anadarko Basin (Figure 1). The first 27 mi^2 (69 km^2) was shot in 1993. In 1994, 57 mi^2 (145 km^2) were acquired. Both surveys had their primary objectives below the Red Fork Formation. In 1996, 67 mi^2 (171 km^2) were acquired with the main objective of imaging the Upper Red Fork incised valley system (which was used in this study). The dominant frequency of the seismic data ranges from 50 Hz up to 80 Hz.

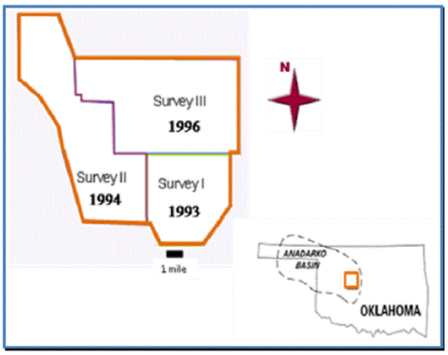

Figure 1. Location map of three surveys in the Anadarko Basin in Oklahoma, showing the year in which they were acquired (After, Del Moro et al., 2009). In this paper, the 3D dataset which was acquired in 1996 will be examined.

The Red Fork Formation is a channel system formed during the Desmoinesian and consists of both sandstone and shale intervals. The Red Fork Formation overlays the regionally extensive Inola and Novi Limestone intervals from the Atoka Group and is superposed by the Pink Limestone from of the Cherokee Group. The Red Fork Zone is characterized by three coarsening upward marine parasequences (Lower, Middle, and Upper Red Fork). The Lower Red Fork is mainly deep-marine shale and siltstone. The Middle Red Fork is marine dominated and was deposited into a relatively deep basin on a steep, unstable delta-front slope and finally the Upper Red Fork deposited in shallower water is a deltaic sequence more fluvial dominated. In this paper, we will focus on the Upper Red Fork incised valley system that consists of multiple stages of incision and fill and contains the best reservoir rocks in the region.

Applying an adaptive subtraction technique to suppress the acquisition footprint pattern as seen on geometric attributes: A Red Fork Formation case study.

Downloaded 01/29/13 to 129.15.127.245. Redistribution subject to SEG license or copyright; see Terms of Use at http://library.seg.org/

Seismic Processing

Seismic data processing plays a vital role in enhancing the signal-to-noise ratio in order to provide better quality data for interpretation. To address acquisition footprint, we reprocessed the Survey III to remove the noise part and to enhance the data quality. Figures 2 and 3 indicate two processing steps that we applied in order to eliminate the background noise from the data and to enhance signal embedded in background noise. Figure 2 shows the stacked section before and after applying F-X deconvolution. F-X deconvolution made reflections significantly easier to recognize, and reduce the noise. Figure 3 shows the migrated section before and after applying a median filter. The median filter further boosted the signal-to-noise ratio and removed the background noise.

Acquisition Footprint Suppression

After attenuating the noise and boosting the signal components of the seismic data, we applied an adaptive subtraction footprint suppression workflow proposed by Falconer and Marfurt (2008) that uses attributes to characterize the footprint. First, the processor chooses an attribute that is particularly sensitive to the footprint. Then, vertically-aligned footprint is enhanced and horizontal stratigraphy suppressed through a vertical median filter (Figure 4). In our study we found the most-positive curvature to be severely contaminated by acquisition footprint. We therefore used it to design our adaptive subtraction footprint suppression workflow. We then characterized the footprint in the k_x-k_y domain, reconstructed the noise in the x-y domain and adaptively subtracted the noise from the original seismic amplitude data for each and every time slices. Finally, we recomputed the attributes from the filtered data and looked for improved imaging of geological features.

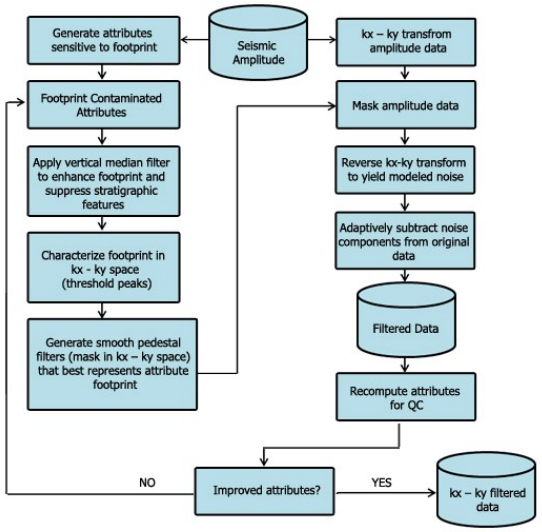

Figure 4. The attribute-driven footprint suppression workflow used in this paper. After Falconer and Marfurt (2008).

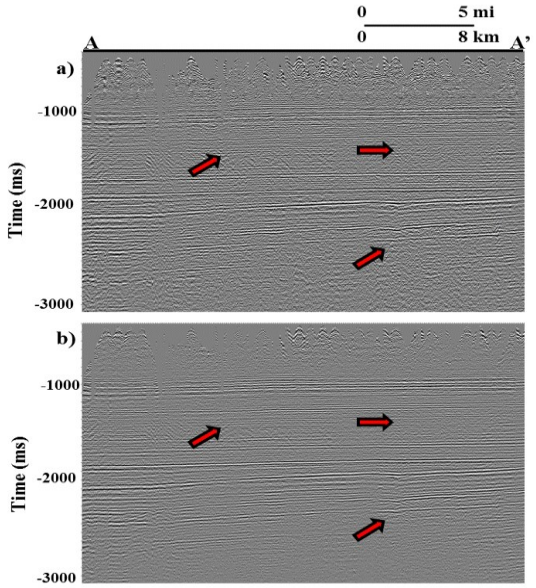

Figure 2. The stacked section a) before and b) after F-X deconvolution. Note that the significant reduction of the noise and enhancement of the coherent signal in the section after applying F-X deconvolution (red arrows).

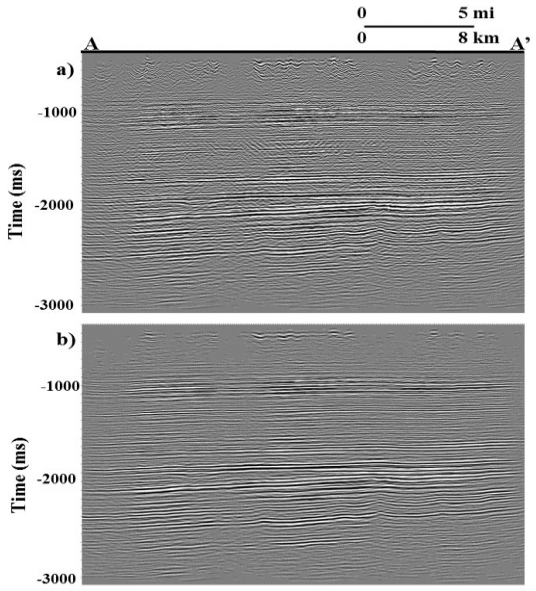

Figure 3. Migrated section a) before and b) after applying the median filter. The median filter results in a cleaner background and focuses amplitudes of the seismic reflections.

Seismic Attribute Analysis and Interpretation

Incised valleys are best picked by using phantom horizons tied to a more continuous, easily-picked reference horizon, which for us was the Skinner. Figure 5 shows phantom horizon slices through seismic amplitude before and after filtering through the Red Fork channels interval 92 ms below the Skinner Horizon. Note the difference in footprint contamination. Seismic attributes represent any measure of seismic data that helps to better visualize or quantify features of

Downloaded 01/29/13 to 129.15.127.245. Redistribution subject to SEG license or copyright; see Terms of Use at http://library.seg.org/

interpretation interest. Three-dimensional data allows the interpreter to view the data either in time slices or horizon slices.

Curvature

Curvature attributes are able to delineate subtle faults, folds, flexures, and in our case, differential compaction over channel systems. Most positive and most negative principal curvatures best define the structural and stratigraphic events. Figure 6 shows the phantom horizon slices at the Red Fork level 92 ms below Skinner Horizon through the most-positive principal curvature. Note that after acquisition footprint suppression, the curvature attributes show not only the edges of the incised valley system, but also indicates potential edges of overbank deposits.

Coherent Energy

While most-positive principal curvature is more commonly used to map structural deformation and depositional components, amplitude–based "attributes" such as RMS amplitude and coherent energy are routinely used to interpret lithology, porosity, and fluid presence. Coherent energy as computed in this study is the square of the envelope of the coherent component of the data within a 3-trace by 3-trace by 20 ms window. Figure 7 shows how effectively the coherent energy can distinguish the channel edges after acquisition footprint suppression.

Coherent Energy Gradient

Coherent energy gradients measure lateral amplitude changes along structural dip and azimuth of only the coherent component of the seismic data. The advantage of coherent energy gradients is that values will be large when there is varying high amplitude coherent energy, and small when the reflectivity is either smoothly varying, low amplitude, or incoherent. For purposes of this study, we found the inline gradient attribute to be highly effective in delineating channel systems. Figure 8 shows that coherent energy gradient delineates both channel edges and channel boundaries after acquisition footprint suppression.

Figure 9 shows phantom horizon slice blending coherent energy and inline gradient attributes at a) 112 ms, b) 102 ms, c) 92 ms, and d) 82 ms below the Skinner horizon. Figure 9a indicates that at 112 ms below the Skinner horizon, white circles display the existence of low coherent energy. Meanwhile, although channel edges can be seen in Figure 5, no clear depositional pattern within the channel is distinguishable with respect to the surroundings. Another flow source can be observed where deposits are coarser clastics north of the channel although the flow conduit itself filled with finer clastics as indicated by low coherent energy. Moreover, once phantom slices are approaching to the Red Fork level (Figures 9b, 9c, and 9d), the existence of high coherent energy is evident (white circles). Therefore, due to the fact that Red Fork channel system consists of sandstone-shale sequence, low coherent energy can be interpreted as finer clastics, while high coherent energy areas can be interpreted as coarser, sandier clastics. The middle area of the channel system show low coherent energy at each horizon slices (black circle) which can be demarcated as finer clastics deposits. This area can be interpreted as erosion where finer clastics were deposited by other channels. Channel edges show high coherent energy in all the places except the area where we interpret the erosional event.

Conclusions

Acquisition footprint is present in all types of seismic data and masks the subtle features. Hence, footprint removal is useful for land data since it enhances the signal-to-noise ratio and suppresses artifacts from the data. In this paper, we have shown how effectively an adaptive subtraction technique suppresses the footprint pattern from the data. The essential fact is that to select the best attributes that sensitive acquisition pattern. In our study, the most-positive principal curvature attribute that best defines footprint pattern was selected. In this paper, we have found that coherent energy and inline gradient attributes best delineate architectural elements of the depositional system. Though coherent energy shows good delineation of the cutbank, the inline coherent energy gradient better delineates point bars and other more subtle (gradational) changes. Furthermore, blending coherent energy with coherent energy gradient components using opacity highlights sand-prone areas within the channel system.

Acknowledgments

The first author wishes to thank the Turkish Petroleum Corporation for their sponsorship of his graduate studies. We thank Chesapeake Energy for their support in this research effort, the industrial sponsors of the AASPI consortium, and Dr. Tim Kwiatkowski, Oswaldo Davogustto, and Kui Zhang for their valuable contribution and feedback.

References

Del Moro, Y., Y. Suarez, and K. J. Marfurt, 2009, Seismic modeling of incised valley fills of the Red Fork Formation in the Anadarko Basin… A way to resolve invisible channels: 79th Annual International Meeting of the SEG, Expanded Abstract, 2632-2636.

Falconer, S., K. J. Marfurt, 2008, Attribute-driven footprint suppression: 78th Annual International Meeting of the SEG, Expanded Abstract, 2667-2671.

Marfurt, K. J., R. M. Scheet, J. A. Sharp, and M. G. Harper, 1998, Suppression of the acquisition footprint for seismic sequence attribute mapping: Geophysics, **63**, 1024-1035.

Peyton, L., R. Bottjer, and G. Partyka, 1998, Interpretation of incised valleys using new 3-D seismic techniques: A case history using spectral decomposition and coherency: The Leading Edge, **17**, 1294-1298.

Downloaded 01/29/13 to 129.15.127.245. Redistribution subject to SEG license or copyright; see Terms of Use at http://library.seg.org/

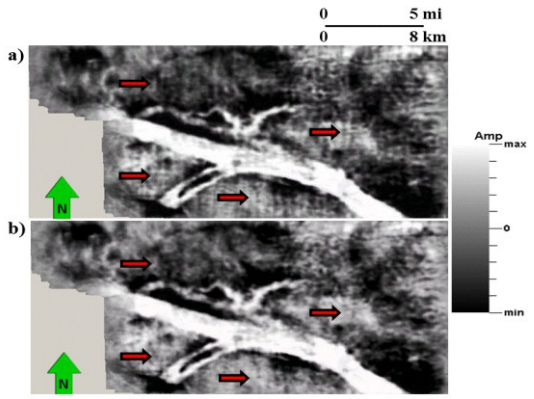

Figure 5. Phantom horizon slices at Red fork level 92 ms below the Skinner Horizon through the seismic amplitude volume a) before and b) after acquisition footprint suppression. Note that acquisition footprint pattern has been suppressed from the data (red arrows).

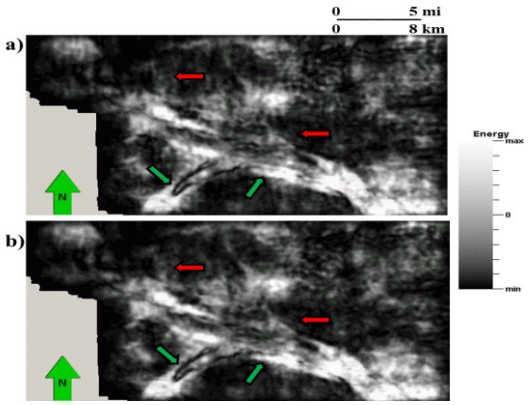

Figure 7. Phantom horizon slices at Red fork level 92 ms below the Skinner Horizon through the coherent energy a) before and b) after acquisition footprint suppression. Note that acquisition footprint pattern has been suppressed from the data (red arrows) and channel edges can be seen clearly (green arrows).

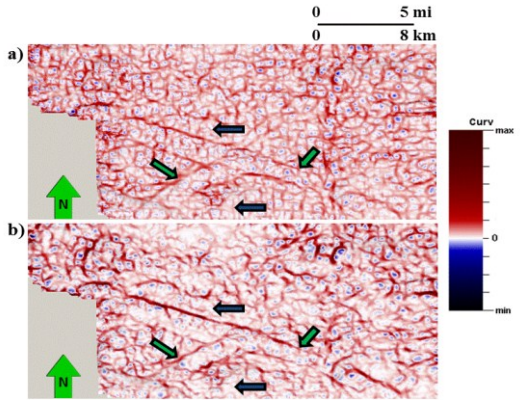

Figure 6. Phantom horizon slices at Red fork level 92 ms below the Skinner Horizon through the most-positive principal curvature a) before and b) after acquisition footprint suppression. Note that acquisition footprint pattern has been suppressed from the data (blue arrows) and Red Fork channel boundaries can be easily distinguished (green arrows).

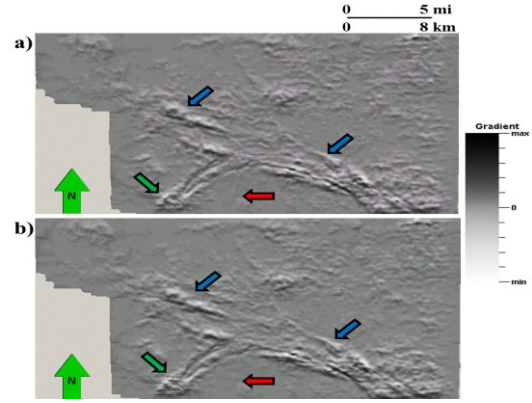

Figure 8. Phantom horizon slices at Red Fork level 92 ms below the Skinner Horizon through inline energy gradient a) before and b) after acquisition footprint suppression. Note that acquisition footprint pattern has been suppressed from the data (red arrow). Channel edge (green arrow) and channel boundaries (blue arrows) can be distinguished easily.

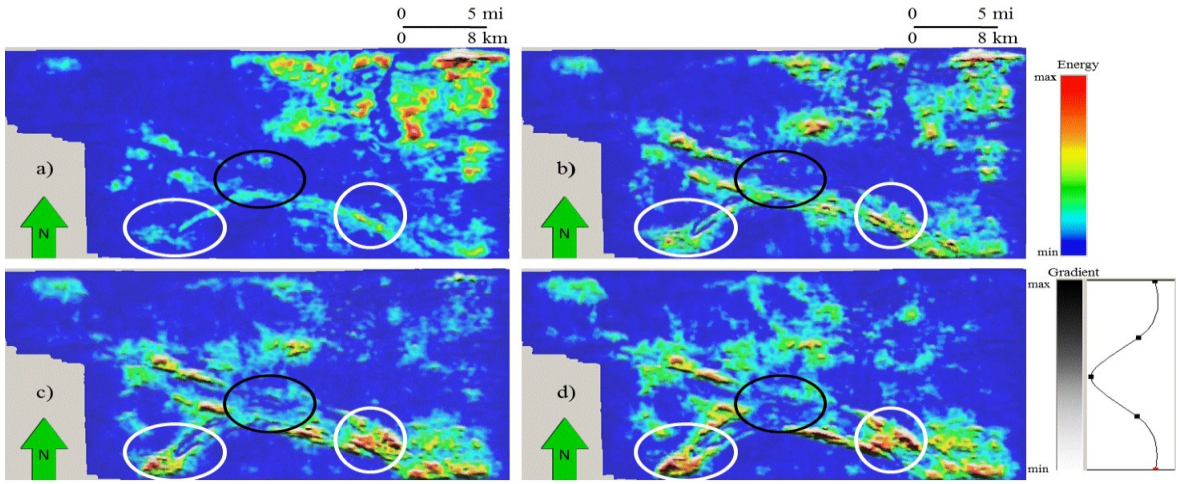

Figure 9. Phantom horizon slices blending coherent energy and inline gradient attributes a) 112 ms, b) 102 ms, c) 92 ms, d) 82 ms below the Skinner horizon. High energy anomalies (white ellipses) to be sand stringers embedded in a shale matrix. Hence, it would be wise to predict little sand near the avulsion point of the channel (black ellipses).